J. Fluid Mech. (1975), *vol.* 71, *part* 3, *pp.* 601–623
Printed in Great Britain

Forced plumes and mixing of liquids in tanks

By A. E. GERMELES

Corporate Research Department, Cabot Corporation,
Billerica, Massachusetts 01821

(Received 3 January 1975 and in revised form 15 May 1975)

We consider the mixing between two miscible liquids of slightly different density ($< 10\%$) when one of them (cargo) is injected into a tank partially filled with the other (inventory). The injection of the cargo is such that buoyancy and inertia act in concert on the plume produced by the cargo. The two basic processes that govern the mixing of the two liquids in the tank are the entrainment of tank liquid by the plume and the tank circulation set up by this entrainment and by the plume discharge. Unlike plumes in an environment of infinite extent, the plume in this case changes its environment continuously, which, in turn, has a continuously-varying effect on the plume. A mathematical model for the mixing of the two liquids is presented, from which one can compute the tank stratification that may result when given amounts of cargo and inventory are thus mixed. Plume entrainment theory is used for the plume dynamics and a 'filling-box' model is used for the tank circulation. The partial differential equations of the model are integrated by an original and unique numerical method. The problem was also treated experimentally. The tank stratification is expressed in terms of a normalized density-difference variable δ. Except for some very localized large discrepancies, due to certain local effects not included in the model, computed and experimental profiles of δ agree very well, their maximum and average deviations being within 4 and 2%, respectively. It is found that values of the empirical plume parameters α and λ that are used commonly for steady plumes in environments of infinite extent are approximately right for the time-dependent plumes under consideration too.

1. Introduction

1.1. *Description of problem and previous work*

The work of this paper resulted from research efforts aimed at the understanding and control of an undesirable event that has occurred in several storage tanks for liquefied natural gas (LNG). The event has come to be known as tank 'roll-over'. LNG storage tanks are operated at about ambient pressure, and some of them are as large as a football field in cross-sectional area. LNG tank roll-over produces an almost spontaneous boil-off of large amounts of methane vapour. The consequent tank over-pressure, sometimes unexpectedly large, is usually relieved by the prompt opening of safety vents. The dynamic processes that lead to LNG tank roll-over are not yet fully understood, at least not in quantitative terms. But one thing about this phenomenon is well established. Its cause is tank stratification

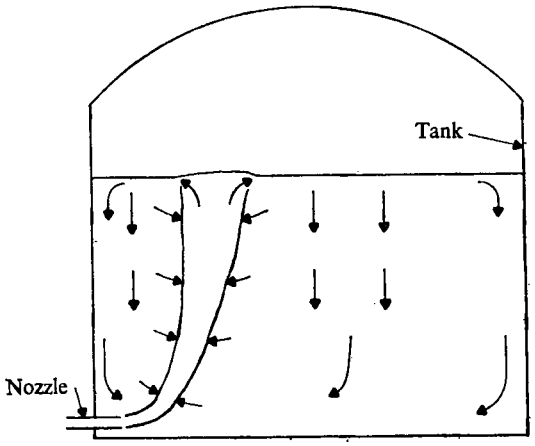

FIGURE 1. Sketch of plume resulting from the addition of light cargo through a horizontal bottom-fill nozzle. Arrows show plume entrainment, discharge of plume, and consequent tank circulation.

that results when an LNG cargo is added to a partially filled tank; the density of the cargo is different from that of the tank's inventory; and cargo and inventory are not mixed adequately during the cargo transfer. Thus, the mixing of cargo with inventory is crucial for LNG tank roll-over. (Besides density stratification, temperature stratification plays an important role in the dynamics of LNG tank roll-over. The latter develops, during the dynamics of roll-over, from density stratification and from normal heat leak into the tank; but it can also arise, partly, from initial temperature differences between cargo and inventory.)

Most operational LNG storage tanks have a single nozzle for the transfer of cargo. This is at the top or bottom of the tank. The injected cargo produces a buoyant jet or forced plume. Mixing of cargo with tank liquid comes about through entrainment of the latter by the plume and through the tank circulation pattern set up by this entrainment and by the plume discharge. These processes are shown schematically in figure 1, which depicts a transfer of light cargo through a horizontal bottom-fill nozzle. Upon completion of the transfer of a given amount of cargo, liquid near the free surface will be lighter than that near the bottom of the tank, and the tank will in general have some stratification, the degree of which depends on a number of factors: density difference between and relative amounts of cargo and inventory, volume and momentum fluxes of the nozzle, and nozzle orientation and configuration. A similar situation results when heavy cargo is transferred through a top-fill nozzle. Note that in both cases buoyancy and inertia act in concert, the plume penetrates the entire liquid level at all times, and therefore all the tank liquid is involved in the mixing process throughout the cargo transfer.

A quite different situation may arise when heavy cargo is transferred through a bottom-fill nozzle (or light cargo through a top-fill nozzle). In such cases, buoyancy and inertia do not act in concert, and the plume will not reach the top (or bottom) of the tank if the cargo does not have sufficient momentum; the plume will spread out into the tank liquid before it reaches the top (or bottom). The

part of the tank liquid which is not penetrated by the plume will remain completely unmixed and, upon completion of the cargo transfer, the tank will have a stable gross stratification.

For further details on LNG tank stratification consequent to various filling procedures, the reader is referred to Smith & Germeles (1974). In that paper, some typical results were presented from a theoretical method for computing the tank stratification. In the present paper, we describe in detail the hydrodynamic and mathematical aspects of the method. Only those cases in which buoyancy and inertia act in concert are covered in this paper. The method is not restricted to LNG's; it is valid for any two liquids, of slightly different density, that are miscible. It is based on a mathematical model for the two basic hydrodynamic processes which, as mentioned above, govern the mixing in the tank: plume entrainment and tank circulation.

A well-accepted mathematical theory for plume entrainment has been developed over the last twenty or so years. Morton, Taylor & Turner (1956) introduced the fundamental hypothesis of plume entrainment: the entrainment at any height along the plume is proportional to a characteristic velocity there. The hypothesis introduced the empirical entrainment constant α. With this hypothesis, a Boussinesq-type approximation, and invoking similarity for the velocity and buoyancy profiles, Morton *et al.* developed a mathematical model for vertical plumes in uniform or stratified environments of infinite extent, and computed some special cases. But they did not incorporate in their model the fact that scalar profiles (like temperature or density) spread differently from velocity profiles, which was shown earlier through the experiments of Rouse, Yih & Humphreys (1952). The different spread of velocity and scalar profiles was subsequently introduced into the model by Morton (1959). This brought a second empirical constant, λ, into plume entrainment. With the revised model, Morton derived a number of interesting results, mostly for a uniform environment. It should be pointed out that, even at this level, the plume entrainment model is so complex that analytic solutions are not possible for any initial conditions on plume mass, momentum and density deficiency, even when the environment is uniform. Fan (1967) and Fan & Brooks (1969) introduced plume inclination into the model, for plumes in environments of infinite extent, and developed computer programs to obtain numerical solutions. In an environment of infinite extent, the plume discharge does not influence the environment and, thus, the governing equations of the model are ordinary differential equations; the independent variable is a space co-ordinate measured along the plume axis.

When the environment is finite (e.g. a finite tank), the plume discharge changes the environment continuously, which, in turn, has a continuously-varying effect on the plume. Then time is also an independent variable, and the governing equations of the problem are now partial differential equations, which increases the mathematical complexity of the problem considerably. For confined and thus changing environments, the plume model must be coupled with a model for the environment. Baines & Turner (1969) proposed a simple model for the environment, which is referred to by Turner (1973) as the 'filling-box' model.

The mathematical model of this paper is basically a combination of the most

recent plume entrainment model used by Fan & Brooks (1969) and of the tank circulation (filling-box) model proposed by Baines & Turner (1969). No previously published work involving plumes in finite environments is based on a model which contains simultaneously as many features and effects as that of this paper. For instance, Baines & Turner did not consider in their model the effects of nozzle inclination (inclined plumes), of mass addition to the filling box, or of initial momentum in the plume. Furthermore, the only time-dependent solution that Baines & Turner computed for their problem is what they call the 'large-time, asymptotic state'. The model described in this paper, in its most general form, has been simulated successfully in a computer program by an original and unique numerical method for the integration of the governing partial differential equations.

LNG tank stratification was also studied at Cabot Corporate Research through modelled laboratory experiments, with scaled-down tanks and nozzles, and with clear water and brine for the two liquids. Typical results from these experiments are included in this paper, to demonstrate the validity of the theoretical model.

1.2. *Outline of the paper*

The theoretical model is presented in §2. To simplify the presentation of the numerical method, we first present the model for a vertical, upward and centred plume in a stratified tank (§2.1) and, on the basis of this model, we then describe in detail the numerical method (§2.2). The modifications of the model for off-centred, inclined and downward plumes are described in §2.3. A brief description of the laboratory experiments is given in §3. Typical results from the theoretical model and from the laboratory experiments are presented, compared and discussed in detail in §4. Finally, in §5 we offer a few concluding remarks.

2. Theoretical model for plumes in tanks

2.1. *Model for vertical, upward and centred plumes*

Consider a cylindrical tank of diameter D, partially filled with a liquid (inventory), with a given stable initial stratification. Assume that another liquid (cargo) of slightly different density from that of the inventory is added to the tank at a volume flux (volumetric flow rate) Q through a round orifice (nozzle) of diameter d located at the centre of the bottom of the tank, as shown in figure 2. Assume, furthermore, that the cargo and the inventory are miscible, and that the cargo is lighter than the inventory, so that the ensuing vertical plume is positively buoyant, and thus penetrates to the free surface of the tank at all times during the cargo transfer. The plume entrains ambient liquid continuously throughout its course, mixes the entrained liquid with its own liquid, and discharges a well-mixed liquid at the free surface. The discharged liquid makes up for the tank liquid entrained by the plume, and also increases continuously the liquid level of the tank. Thus, the entrainment and discharge of the plume set up a circulation pattern in the tank, as shown in figure 2. Obviously, this problem has azimnthal symmetry.

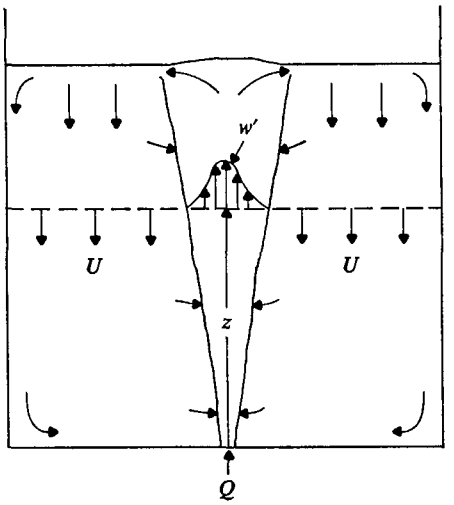

FIGURE 2. Schematic of plume resulting in cylindrical tank from centred bottom orifice discharging at volume flux Q. Shown are plume outline, entrainment and discharge, and consequent tank circulation. Also shown, at station z, are velocity profile w' of plume, and average downward velocity U of tank liquid.

Let z be a space co-ordinate, increasing upward, with its origin at the orifice (figure 2). The instantaneous tank stratification is a function of z and of time t, and the dependent variables of the plume are functions of z, t and a radial co-ordinate r, measured from the plume axis. The equations of conservation of volume, momentum and density deficiency for the plume are, respectively,

$$\frac{\partial}{\partial z}(b^2 w) = 2\alpha b w, \tag{1}$$

$$\frac{\partial}{\partial z}(b^2 w^2) = 2\lambda^2 b^2 \Delta, \tag{2}$$

$$\frac{\partial}{\partial z}(b^2 w \Delta) = \left(1+\frac{1}{\lambda^2}\right) b^2 w \frac{\partial \Delta_a}{\partial z}. \tag{3}$$

b is the effective radius of the plume; w is the axial velocity of the plume evaluated on the plume axis; α is the empirical entrainment constant; λ is an empirical constant for the density profile in the plume; $\rho_0 \Delta$ is the buoyancy of the plume evaluated on the plume axis, ρ_0 being a reference density; and Δ_a pertains to the instantaneous tank stratification, being

$$\Delta_a = g(\rho_a - \rho_0)/\rho_0. \tag{4}$$

g is the acceleration due to gravity; and ρ_a is the instantaneous density profile of the tank. In deriving (1)–(3), we made the usual similarity assumptions for the profiles of the axial velocity of the plume liquid w' and of the plume density ρ; i.e. at any height in the plume, the profiles of w' and of the plume density deficiency are Gaussian:

$$w' = w \exp\left(-\frac{r^2}{b^2}\right) \quad \text{and} \quad g\frac{\rho_a - \rho}{\rho_0} = \Delta \exp\left(-\frac{r^2}{\lambda^2 b^2}\right). \tag{5), (6}$$

Whereas the variables w' and ρ are functions of z, r and t, the variables b, w and Δ are functions of z and t only.

A detailed derivation of (1)–(3) from integral formulations of the conservation equations can be found in Fan (1967), although the equations that Fan derives are for plumes in environments of infinite extent; i.e. for time-independent, steady-state plumes. Here, the plume is time-dependent, owing to the continuous variation of the environment with time, and, in addition to the assumptions made by Fan and others in deriving the plume conservation equations, we made the following: (i) time rates of change can be neglected in the plume conservation equations; (ii) the effective plume diameter $2b$ is, at all times and at all heights, much smaller than the tank diameter D.

For the dynamics of the tank liquid (tank circulation), we adopt the 'filling-box' model proposed by Baines & Turner (1969). It is assumed in the filling-box model that the gross downward motion of the tank liquid, due to plume entrainment, can be described by an average velocity U, as shown in figure 2. (U is, of course, a function of z and t.) Then U must satisfy the volume continuity equation

$$\tfrac{1}{4}\pi D^2 U = \pi b^2 w - Q. \tag{7}$$

The corresponding equation of Baines & Turner does not have the Q term, since in their problem there was no mass addition to the filling box. With the gross motion of the tank liquid described in this way by U, the equation of continuity for the tank liquid is

$$\frac{\partial \Delta_a}{\partial t} - U\frac{\partial \Delta_a}{\partial z} = 0, \tag{8}$$

which is the other equation of the filling-box model. The level of the free surface in the tank is

$$z_n = H_0 + \frac{4Qt}{\pi D^2}. \tag{9}$$

H_0 is the inventory level in the tank; and t is measured from the start of the cargo transfer.

Equations (1)–(3) and (7)–(9) are the governing equations of the model. Let us introduce the normalized variables

$$\left.\begin{aligned} &\zeta = \frac{z}{H_F}, \quad \zeta_n = \frac{z_n}{H_F}, \\ &\tau = \frac{4Qt}{\pi D^2(H_F - H_0)}, \quad q = \frac{\pi b^2 w}{Q}, \quad m = \frac{\pi^2 d^2 b^2 w^2}{8Q^2}, \\ &f = \frac{\pi\lambda^2\rho_0 b^2 w\Delta}{g(1+\lambda^2)(\rho_0-\rho_c)Q}, \quad \delta = \frac{\rho_0-\rho_a}{\rho_0-\rho_c}, \quad u = \frac{\pi D^2 U}{4Q}. \end{aligned}\right\} \tag{10}$$

H_F is the final level in the tank (at the completion of the cargo transfer); and ρ_c is the density of the cargo, which is assumed to be constant. Note that the normalized independent variables of the model τ and ζ are so defined that, at the completion of the cargo transfer, $\tau = 1$ and $\zeta_n = 1$. The normalized dependent

variables of the plume are q, m and f; and they are respectively equal to the plume fluxes of volume, momentum and buoyancy. The normalized dependent variables of the tank liquid are δ and u.

In the normalized variables, the governing equations of the model are

$$\frac{\partial q}{\partial \zeta} = \beta m^{\frac{1}{2}}, \quad \frac{\partial m}{\partial \zeta} = \gamma \frac{qf}{m}, \quad \frac{\partial f}{\partial \zeta} = -q\frac{\partial \delta}{\partial \zeta}, \quad \frac{\partial \delta}{\partial \tau} = hu\frac{\partial \delta}{\partial \zeta}, \tag{11)-(14}$$

$$u = q - 1, \quad \zeta_n = 1 - h(1-\tau). \tag{15), (16}$$

The parameters β, γ and h are defined by

$$\beta = 4\sqrt{2}\,\alpha\frac{H_F}{d}, \quad \gamma = \frac{\pi^2 g(1+\lambda^2)\,d^4 H_F(\rho_0 - \rho_c)}{32\rho_0 Q^2}, \quad h = 1 - \frac{H_0}{H_F}. \tag{17)-(19}$$

The parameter γ is equal to the effective rate of work done by buoyancy, throughout the plume column, divided by the rate of kinetic energy released by the orifice; i.e. γ is an effective Richardson number Ri_0, or the squared inverse of the effective internal Froude number Fr. (See Turner 1973, pp. 12, 176.)

The initial and boundary conditions required for unique solutions of the governing equations are as follows. The required initial condition is that the stratification of the tank inventory must be known; i.e. the initial profile of δ (at $\tau = 0$) must be specified. The required boundary conditions are that the plume fluxes of volume, momentum and buoyancy must be specified at a fixed station for all times. Here, we match these plume variables to those of the orifice flow; thus the boundary conditions are

$$\left.\begin{aligned} q = m = 1 \\ f = 1 - \delta \end{aligned}\right\} \quad \text{at} \quad \zeta = 0 \quad \text{for} \quad \tau \geqslant 0. \tag{20}$$

In specifying (20), we neglect a small flow-development region, through which orifice flow is converted to plume flow. There is one more continuity condition that is imposed on the model: at the free surface, the density of the tank liquid must be equal to the average density of the liquid discharged by the plume. Owing to the density difference between cargo and inventory, this condition introduces at the free surface a step discontinuity in density at $\tau = 0$, when the plume is 'turned on'. The discontinuity moves downward with time. This last condition, and the resulting discontinuity, are discussed in more detail in § 2.2, where the numerical solution of the model is described.

It is important to note that only one of the four partial differential equations of the model contains a derivative with respect to time: namely (14). The method devised for the numerical integration of the differential equations of the model takes advantage of this peculiarity.

2.2. *Numerical solution*

Assume that the profile of δ is known at time τ; and let it be represented by the 'staircase' function

$$\delta = \sum_{i=1}^{n} \delta_i [S(\zeta - \zeta_{i-1}) - S(\zeta - \zeta_i)]. \tag{21}$$

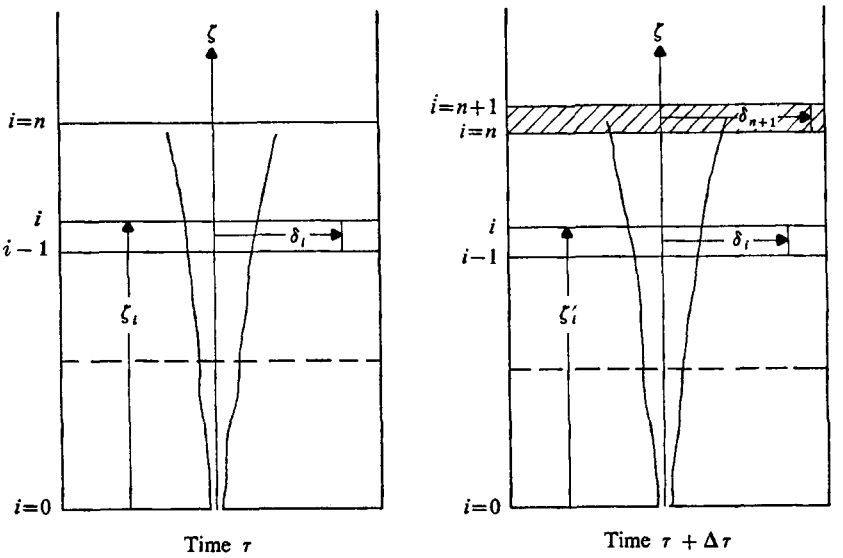

FIGURE 3. Sketch defines staircase structure of δ profile at times τ and $\tau+\Delta\tau$. In time interval $\Delta\tau$, step interfaces move downward from ζ_i to ζ_i', and a new step (hatched) of amplitude δ_{n+1} is added to staircase by discharge of plume. Included are plume outline and position of front (– – –).

S is the unit-step function defined by

$$S(\zeta-\zeta_i) = \begin{cases} 0 & \text{for} \quad \zeta < \zeta_i, \\ 1 & \text{for} \quad \zeta \geqslant \zeta_i. \end{cases} \tag{22}$$

There are n steps in the staircase. The ith step extends from $\zeta = \zeta_{i-1}$ to $\zeta = \zeta_i^-$ (ζ_i^- is smaller than, but arbitrarily close to, ζ_i); and its amplitude is δ_i. (See figure 3.) The values of the array $\delta_i (1 \leqslant i \leqslant n)$ are known; so are the values of the array $\zeta_i (0 \leqslant i \leqslant n)$. ζ_0 is at the origin of the ζ axis (i.e. $\zeta_0 = 0$), while ζ_n is the position of the free surface at time τ, as given by (16).

With this representation of δ, integration of (13) with the boundary conditions for f given by (20) yields

$$f = 1 - \sum_{i=1}^{n} \delta_i [q_{i-1} S(\zeta-\zeta_{i-1}) - q_i S(\zeta-\zeta_i)]. \tag{23}$$

q_i is the value of q at $\zeta = \zeta_i (0 \leqslant i \leqslant n)$. Thus, the profile of f at time τ also has a staircase form. Except for q_0, which must be equal to 1 according to the boundary conditions (20), the values of the array q_i are as yet unknown. An equivalent expression of (23) is

$$f = \sum_{i=1}^{n} f_i [S(\zeta-\zeta_{i-1}) - S(\zeta-\zeta_i)]. \tag{24}$$

f_i is the amplitude of the ith step in the staircase profile of f. It can be shown that, for (23) and (24) to be identical, the f_i's must satisfy the recurrence relation

$$f_i = f_{i-1} - q_{i-1}(\delta_i - \delta_{i-1}), \quad 2 \leqslant i \leqslant n, \tag{25}$$

where f_1 is given by the boundary condition (20); i.e.

$$f_1 = 1 - \delta_1. \tag{26}$$

With f_1 known from (26), (11) and (12) are now integrated forward from $\zeta = \zeta_0 = 0$, where q and m are known from the boundary conditions (20), to $\zeta = \zeta_1$. (A Runge–Kutta integrating scheme is used for this integration in the computer program.) This integration yields the profiles of q and m in the interval $\zeta_0 \leqslant \zeta \leqslant \zeta_1$. With q_1 now known, f_2 is then computed from (25). Next, (11) and (12) are again integrated, from $\zeta = \zeta_1$ to $\zeta = \zeta_2$, and so on to the free surface. This procedure determines the amplitudes f_i of the staircase profile of f and the continuous profiles of q and m at time τ. The profile of u and particularly, the values u_i of u at $\zeta = \zeta_i$ $(0 \leqslant i \leqslant n)$ are then computed from (15). Thus, the profiles of all dependent variables are now known at time τ.

Next, let time be increased by a small interval $\Delta\tau$. In the time interval $\Delta\tau$, the interfaces ζ_i of the staircase profile of δ move downward to new positions ζ_i' (see figure 3), which, to a first approximation, are given by

$$\zeta_i' = \zeta_i - hu_i\Delta\tau, \quad 1 \leqslant i \leqslant n. \tag{27}$$

Thus, the staircase profile of δ is squeezed downward in accordance with (27), while the amplitudes δ_i of the staircase steps remain constant. This process is equivalent to integrating (14) in the time interval $\Delta\tau$. Note that, since u is maximum at the free surface and equal to zero at the bottom of the tank, the squeezing of the staircase becomes progressively more intense from the bottom of the tank to the free surface. Note also that this downward squeezing represents, physically, the entrainment of ambient liquid by the plume in the time interval $\Delta\tau$.

During the same time interval $\Delta\tau$, the plume also discharges a small amount of liquid, shown by the cross-hatched area in figure 3, which becomes part of the tank liquid; i.e. another step of amplitude δ_{n+1}, that extends from ζ_n' to ζ_{n+1}', is added to the staircase profile of δ. It can be shown that, to the approximation on which (27) is based,

$$\delta_{n+1} = \delta_n + f_n/q_n. \tag{28}$$

f_n is the amplitude of the nth step in the staircase profile of f at time τ; and q_n is the value of q at $\zeta = \zeta_n$ and at time τ. Since f_n and q_n are known, (28) determines the value of δ_{n+1}. Also from (16),

$$\zeta_{n+1}' = 1 - h(1 - \tau - \Delta\tau). \tag{29}$$

Thus, the entire staircase profile of δ is now known at time $\tau + \Delta\tau$. It has one step more than it had at time τ; and it is

$$\delta = \sum_{i=1}^{n+1} \delta_i [S(\zeta - \zeta_{i-1}') - S(\zeta - \zeta_i')]. \tag{30}$$

With the profile of δ known at time $\tau + \Delta\tau$, repetition of the procedures described above for the computation of the other dependent variables of the model (f, q, m and u) yields the profiles of these at time $\tau + \Delta\tau$. Since the profile of δ is specified at $\tau = 0$ by the initial condition, repeated applications of the procedures can yield a unique numerical solution at any future time.

After each discharge by the plume, the difference $\Delta\delta$ of the δ values of the two uppermost steps in the staircase profile of δ is given, from (28), by

$$\Delta\delta = f_n/q_n. \tag{31}$$

As the staircase is squeezed downward in time while more steps are added on its top by the consecutive discharges of the plume, the differences $\Delta\delta$ between adjacent steps remain unchanged. Now, these differences $\Delta\delta$ are small in the same sense that the time intervals $\Delta\tau$ are so, except for the first discharge of the plume right after it is 'turned on'. For the first discharge, the ratio f_n/q_n (and hence $\Delta\delta$) can be a large quantity, depending on the density difference between cargo and inventory and on the amount of entrainment by the plume. Thus, the staircase profile of δ can have, in general, one very steep step, which results from the first discharge of the plume and represents a physical discontinuity in the profile of tank stratification. The front edge of this steep step will henceforth be referred to as the 'front'. (Baines & Turner (1969) call a similar discontinuity in their problem the 'first front'.) The front travels downward with time, as shown in figure 3. The discontinuity in δ across the front does not change with time.

The staircase profile of f also has a physical discontinuity at the front. However, unlike that of δ, the discontinuity of f at the front does change with time, since f is a function of the plume density, as well as of the ambient density ρ_a.

A FORTRAN computer program was developed for the model, with the numerical procedures described above. It uses continuously-variable time intervals for the time integration, which it selects by certain criteria. It monitors continuously the heights of the steps in the staircase profile of δ, which decrease continuously as the staircase is squeezed downward with time. If a particular step becomes too low, by certain criteria, it is absorbed by either of the two adjacent to it, in a way that preserves the local average value of δ. Obviously, this periodic elimination of steps is to avoid accumulating a staircase with a prohibitively large, and unnecessary, number of steps. (Recall that a new step is added to the staircase after each time interval.) But the step with the front is excluded from this manipulation, to preserve the exact value of the discontinuity in δ across the front and the exact position of the front with time. The program has other interesting features, description of which is beyond the scope of this paper.

2.3. *Other plume configurations*

The ideal plume configuration (vertical, upward and centred with respect to the tank) of the model of § 2.1 is not usually met in practice. In LNG storage tanks, the fill nozzle (orifice) has quite often an off-vertical orientation, and is usually quite close to the tank wall, too. Thus, the ensuing plume is neither vertical nor centred with respect to the tank. Furthermore, when a cargo that is heavier than the tank's inventory is transferred through a top-fill nozzle, the ensuing plume is still accelerating as in § 2.1, but it is downward instead of upward.

As mentioned earlier, we purposely chose to describe the details of the model in terms of the ideal plume configuration, to simplify the presentation of the numerical method. In this section, we state the modifications of the model of

§2.1 that are required to cover off-centred, inclined and downward plumes. The laboratory experiments, which modelled actual LNG storage tanks, and with which the computer model is compared in §4, involve plume configurations such as the ones described in this section.

2.3.1. *Off-centred and inclined plumes.* One of the basic conditions on which the model of §2.1 is based is that the plume diameter $2b$ must be much smaller than the tank diameter D throughout the plume at all times. This condition excludes interference of the tank wall with the plume. Also, it justifies the validity of the basic feature of the 'filling-box' model for the tank circulation: that the gross downward motion of the tank liquid can be described by an average velocity U.

Consider now the off-centred vertical plume that ensues when a nozzle is not positioned on the centre of the tank. If the plume remains a few plume diameters away from the tank wall throughout its course, so that the wall does not interfere with it, then the model of §2.1 is valid here too, despite our no longer having azimuthal symmetry. But, as is sometimes the case in LNG tanks, the nozzle may be so close to the wall that the wall could interfere with it, at least above a certain plume height. We believe that the model of §2.1 is valid even for such cases, provided that the entrainment constant α is properly reduced, to account for any prominent wall interference effects. (The reduction of α could be made only above a certain plume height, at which wall interference begins.)

Next, consider the inclined plume that ensues when a nozzle is inclined as indicated in figure 1. Again, the basic principles of plume entrainment and tank circulation used in the model of §2.1 are valid here, provided the plume path is such that the wall does not interfere with the plume. We shall not present here a complete exposition of the model with inclined plumes. A detailed derivation of the equations of inclined plumes in environments of infinite extent can be found in Fan (1967). Instead, we shall simply describe the few alterations of the governing equations of the model of §2.1 that are introduced by plume inclination.

Let θ be the inclination of the plume axis with respect to the horizontal plane, and θ_0 be the value of θ at the nozzle (i.e. the nozzle inclination). Make the following single modification to the normalized variables defined by (10):

$$m = \frac{\pi^2 d^2 b^2 w^2}{8Q^2} \sin\theta. \tag{32}$$

m is still equal to the flux of vertical momentum in the plume. Then it can be shown that the only alteration of the normalized conservation equations of the plume (11)–(13) is that (11) must be replaced by

$$\frac{\partial q}{\partial \zeta} = \beta m^{\frac{1}{2}} (1 + \cos^2\theta_0/m^2)^{\frac{1}{4}}. \tag{33}$$

This equation, as well as (34) and (36) below, can be derived readily when it is recognized that the flux of horizontal momentum in the plume must remain constant, since the only external forces that act on the plume (buoyancy or gravity) are vertical. The path of the plume can be computed from

$$\frac{\partial \chi}{\partial \zeta} = \frac{\cos\theta_0}{m}. \tag{34}$$

χ is the horizontal co-ordinate of the plume axis normalized by H_F. The boundary condition on χ is

$$\chi = 0 \quad \text{at} \quad \zeta = 0 \quad \text{for} \quad \tau \geqslant 0. \tag{35}$$

The inclination of the plume can be computed from

$$\sin\theta = (1 + \cos^2\theta_0/m^2)^{-\frac{1}{2}}. \tag{36}$$

As for the equations for the tank liquid (tank circulation), it can be shown that (14) and (15) are still valid except in a small region near the bottom of the tank when the nozzle is horizontal (see also the discussion below). The only alteration of the boundary conditions given by (20) is that

$$m = \sin\theta_0 \quad \text{at} \quad \zeta = 0 \quad \text{for} \quad \tau \geqslant 0. \tag{37}$$

In summary, the normalized equations of the model with inclined plumes are (12)–(16), (33) and (34). The normalized boundary conditions are given by (20), as modified by (37), and (35). The initial condition and the continuity condition at the free surface are the same as in the model of § 2.1.

No basic alterations of the numerical procedures of § 2.2 are needed with inclined plumes. The plume path can be found readily by integrating (34) with the boundary condition (35). However, when the nozzle is horizontal ($\theta_0 = 0$), the governing equations have a singularity at $\zeta = 0$, as may be seen from (37), (12), (33) and (34). Numerically, this difficulty can be taken care of readily, by using a value of θ_0 that is slightly larger than zero (by one or two degrees).

The physical ramifications of a horizontal nozzle are as follows. If the cargo jet is very strong, it can travel a considerable distance along the bottom of the tank before being bent upwards by buoyancy, becoming an inclined forced plume. This local effect is not included in the model, and therefore the model cannot predict the tank stratification in a small region near the bottom of the tank for such a case. But the model is valid outside this small region. For weak cargo jets, the cargo becomes an inclined buoyant plume within a few nozzle diameters of the nozzle; hence, this local effect is insignificant. (It is assumed that there is a significant density difference between cargo and inventory.)

For inclined plumes, Ri_0 is equal to γ divided by the square of the value of m at $\zeta = 0$ given by (37).

2.3.2. *Downward plumes.* Consider now the transfer into a tank of a cargo which is heavier than the tank's inventory, through a top-fill nozzle. The resultant downward plume is again an accelerating plume. Let us assume that the nozzle is above the free surface of the tank liquid throughout the cargo transfer. It can be shown readily that the model for upward plumes, with a slight alteration of the boundary conditions, applies also to downward plumes, provided that the origin of the ζ co-ordinate is taken on the moving free surface with ζ increasing downward, and that g is replaced by $-g$. ζ_n now becomes the instantaneous position of the bottom of the tank, which moves away from the origin of ζ (free surface) as the tank is filled up.

Alteration of the boundary conditions is required by the cargo jet's free fall, which increases its vertical momentum. On the assumption that it does not break

up during fall, its momentum at $\zeta = 0$ can be computed readily from Bernoulli's equation. Then, at $\zeta = 0$ for $\tau \geqslant 0$, the boundary conditions for m and χ are

$$m = \left[\sin^2\theta_0 + 2\gamma_1\left(1 - \frac{h}{h_1}\tau\right)\right]^{\frac{1}{2}}, \tag{38}$$

$$\chi = \frac{h_1}{\gamma_1}\cos\theta_0\left\{-\sin\theta_0 + \left[\sin^2\theta_0 + 2\gamma_1\left(1 - \frac{h}{h_1}\tau\right)\right]^{\frac{1}{2}}\right\}. \tag{39}$$

The parameters γ_1 and h_1 are defined by

$$\gamma_1 = \frac{\pi^2 g H_1 d^4}{16Q^2}, \quad h_1 = \frac{H_1}{H_F}. \tag{40), (41}$$

H_1 is the height of the nozzle above the free surface at $\tau = 0$. γ_1 is the squared inverse of the effective Froude number for the free fall at $\tau = 0$. Note that m and χ at $\zeta = 0$ decrease with time, in this case.

In the boundary condition (38), it is assumed that there is no surface-entry effect on the momentum of the cargo jet. The laboratory experiments with top-fill nozzles showed that the jet from an inclined nozzle produces a great number of surface waves and much agitation as it enters the tank liquid, while the jet from a vertical nozzle ($\theta_0 = 90°$) makes a very smooth entry, with hardly noticeable waves. Surface agitation and waves consume energy that must come from the jet: the momentum of the jet is reduced. Thus, the boundary condition (38) on m is not accurate when the nozzle is inclined.

Ri_0 is equal to γ divided by the square of the value of m at $\zeta = 0$ as given by (38). Since m at $\zeta = 0$ decreases with time, Ri_0 increases with time in this case.

3. Brief description of laboratory experiments

Figure 4 is a schematic of the apparatus with a top-fill nozzle. Clear water and brine were used for the two liquids. Cargo of a specified density was first prepared in a large stainless-steel cylindrical tank, then transferred through a nozzle to a cylindrical Plexiglas tank, of diameter 4 ft, which held a specified amount of inventory. The density difference between cargo and inventory was usually less than 7 %. The cargo was coloured with methylene blue, to facilitate visual observations and photographing of the plume and mixing processes in the Plexiglas tank.

The cargo transfer pump had a constant flow rate. A needle valve was used to set the desired cargo flow rate, and most of the pump's throughput was discharged back into the cargo tank, thus keeping the cargo well mixed at all times. The cargo flow rate was measured with a rotameter.

Upon completion of a cargo transfer operation, the stratification profile of the Plexiglas tank was taken by drawing samples from various depths of the tank with a probe. Figure 4 includes a schematic of the probe assembly. The probe was made from plastic and copper tubing, a syringe, a graduated length scale and a $\frac{1}{2}$ in. diameter steel ball with the intake orifice. The ball was connected to the syringe with plastic tubing, most of which was inserted into a straight section of copper tubing. The ball was attached to the end of the copper tubing permanently.

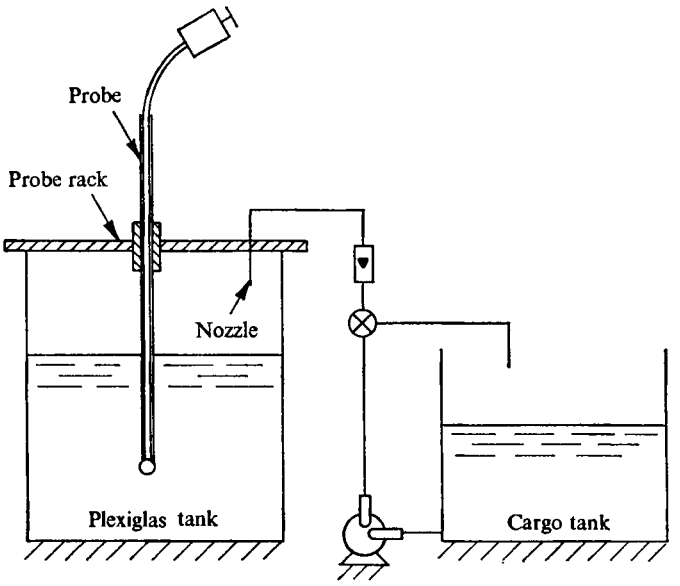

FIGURE 4. Schematic apparatus with top-fill nozzle.

The length scale was attached to the side of the copper tubing. A rack at the top of the Plexiglas tank (figure 4) was used to insert the probe to and hold it at a desired depth. A sample having been drawn into the syringe, the probe was drawn out of the tank, the sample was transferred to a container, and the probe was flushed thoroughly with air. (The syringe had a valve for this purpose.) The rack constrained the movement of the probe to the vertical direction, minimizing disturbances of the tank liquid. The depth from which a sample was drawn was read off on the length scale attached to the probe. The specific gravity of each sample was measured with an analytical balance and a standard 25 cc flask commonly used for specific gravity measurements of liquids.

This technique for measuring tank stratification profiles was developed and improved through a number of series of experiments. For the most recent series of experiments, it is estimated that the accuracies of the depth and specific gravity measurements are at least $\frac{1}{32}$ in. and 0·0001, respectively.

4. Results and discussion

A number of cases were both modelled in the laboratory and simulated by the computer program. The computed and experimental results for two typical cases are now presented and discussed.

One obvious problem in the computer simulations was the choice of appropriate values for the empirical constants α and λ, in view of the fact that the values for plumes differ from those for jets. Morton (1959) pointed out the distinction between a jet and a plume. An ideal jet is characterized by constant momentum throughout its course (no buoyancy forces, $Fr = \infty$). An ideal plume is characterized by no initial momentum ($Fr = 0$); its momentum is acquired through the action of buoyancy. Anything between these two ideal extremes is a

Parameter	Example §4.1	Example §4.2
Tank diameter D (ft)	4	4
Inventory level H_0 (in.)	16.69	2·03
Final level H_F (in.)	28.80	2·70
Cargo flow rate Q (g.p.m.)	1·11	0·0718
Nozzle diameter d (in.)	0·53	0·40
Nozzle orientation θ_0 (deg.)	90	0†
Initial height of nozzle above free surface H_1 (in.)	17·61	NA
Inventory density ρ_0 (sg)	0·9988	1·0582
Cargo density ρ_c (sg)	1·0584	0·9979
Entrainment constant α	0·082	0·082
λ	1·16	1·16
β	25·21	3·131
γ	2·074	1·440
h	0·4205	0·248
γ_1	18·12	NA
h_1	0·6115	NA
Fr	4·23‡	0·0291

† $\theta_0 = 2°$ was used in the computer program.
‡ At the onset of the cargo transfer ($\tau = 0$).

TABLE 1. Summary of parameters

'buoyant jet' or a 'forced plume', and this is precisely what we have here. For round ideal plumes, $\alpha = 0{\cdot}082$ and $\lambda = 1{\cdot}16$; for round ideal jets, $\alpha = 0{\cdot}057$ and $\lambda = 1{\cdot}12$. It is common practice to use in forced plumes the values of α and λ for ideal plumes. Thus, unless stated otherwise, the values of α and λ used throughout this work are 0·082 and 1·16, respectively.

4.1. *First example*: *top-fill, vertical nozzle*

In this case, cargo heavier than the tank's inventory by 5·97 % is transferred through a top-fill nozzle directed straight down. The physical and normalized parameters of the case are summarized in table 1. Included in table 1 is the value of Fr at the onset of the cargo transfer ($\tau = 0$). The tank is unstratified initially, and the reference density ρ_0 is taken to be equal to the inventory density, so that $\delta = 0$ initially. The nozzle is far enough away from the tank wall that there is no significant wall interference with the plume. This was observed visually in the laboratory, and also was predicted by the computer program, which computed the effective plume diameter throughout the course of the plume.

Figures 5 and 6 show the fluxes of volume q and momentum m in the plume as functions of time τ and distance from the free surface of the tank ζ. (Recall that $\tau = 1$ corresponds to the completion of the cargo transfer and that, with top-fill nozzles, the origin of ζ is attached to the free surface.) Note that the plume entrains, per unit time, 40 (at $\tau = 0$) to 56 (at $\tau = 1$) times its initial volume. Owing to the free fall, the momentum of the cargo jet is multiplied by a factor of 6·1 (at $\tau = 0$) to 3·5 (at $\tau = 1$) by the time the jet hits the free surface. After the entry of the jet into the tank liquid, the momentum flux m of the ensuing

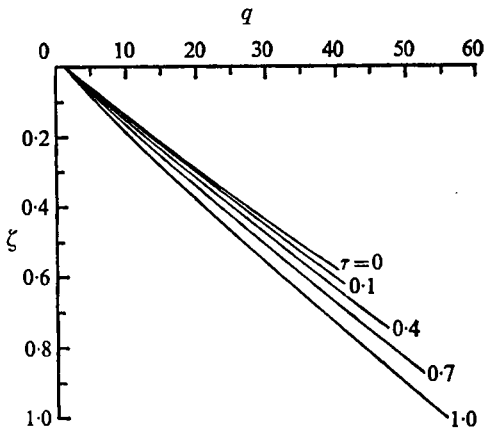

FIGURE 5. Example §4.1: volume flux q against distance from free surface ζ for various times τ.

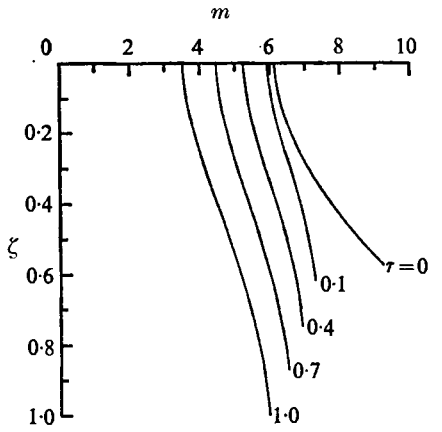

FIGURE 6. Example §4.1: momentum flux m against distance from free surface ζ for various times τ.

plume is increased continuously by the net downward gravity forces. But, as figure 6 shows, the change of m with ζ is relatively slow near the free surface. This is a consequence of the fact that Fr is rather large throughout the cargo transfer; Fr is equal to 4·23 and 2·43 at $\tau = 0$ and $\tau = 1$, respectively.

The computed tank stratification profiles δ for various times and the corresponding fluxes of plume buoyancy f are shown in figures 7 and 8. The staircase structure of both δ and f is an artifact of the numerical method. By the time $\tau = 0{\cdot}1$, the front has already moved to $\zeta = 0{\cdot}036$ (i.e. near the free surface). This is a consequence of the high speed with which the front moves upwards in this case; q, and therefore u, is very large away from $\zeta = 0$, as shown in figure 5. But it can be shown that an infinite time is required for the front to arrive exactly on the free surface, although here the front is very close to the free surface by the time about 20% of the cargo has been transferred ($\tau = 0{\cdot}2$). The step discontinuity in δ aeross the front is only 0·0249 (very small). This is also a conse-

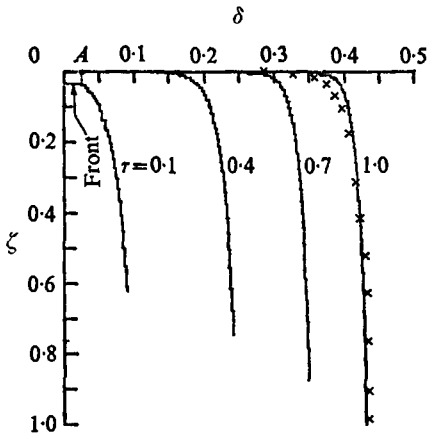

FIGURE 7. Computed tank stratification profiles in example §4.1 for various times τ. Free surface is at $\zeta = 0$. After cargo transfer ($\tau = 1$), bottom of tank is at $\zeta = 1$. Point A, very close to the free surface, is origin of δ profiles at $\tau = 0{\cdot}4$, $0{\cdot}7$ and 1. ×, experimental profile at $\tau = 1$.

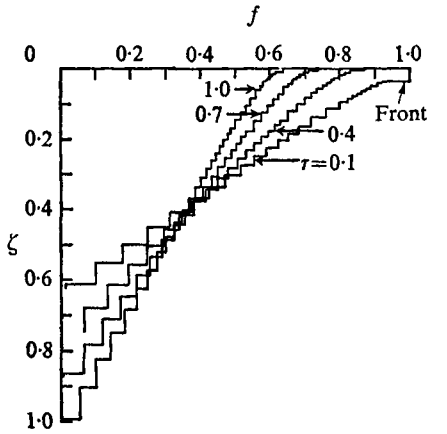

FIGURE 8. Example §4.1: buoyancy flux f against distance from the free surface ζ for various times τ.

quence of the large q. That is to say, so much more ambient liquid is entrained by the plume than is in the cargo jet, that the first discharge of the plume (at $\tau = 0$) has a δ only slightly different (by only 0·0249) from that of the inventory. The profiles of δ and f behind the front become continuously steeper as the front advances toward the free surface. In fact, by the time the front gets very close to the free surface ($\tau = 0{\cdot}2$), the profile of δ very near the front becomes so steep that it is impossible to draw it on the scales of figure 7. In figure 7 the origin of the δ profiles at $\tau = 0{\cdot}4$, $0{\cdot}7$ and 1 is depicted as point A, which has a value of δ equal to 0·0249 and a very small value of ζ that decreases continuously with time, but cannot become exactly equal to zero in a finite time.

Included in figure 7 is the tank stratification profile that was obtained in the laboratory after cargo transfer. The experimental tank stratification is stable and also very smooth, an indication of the accuracy of the measurements. The

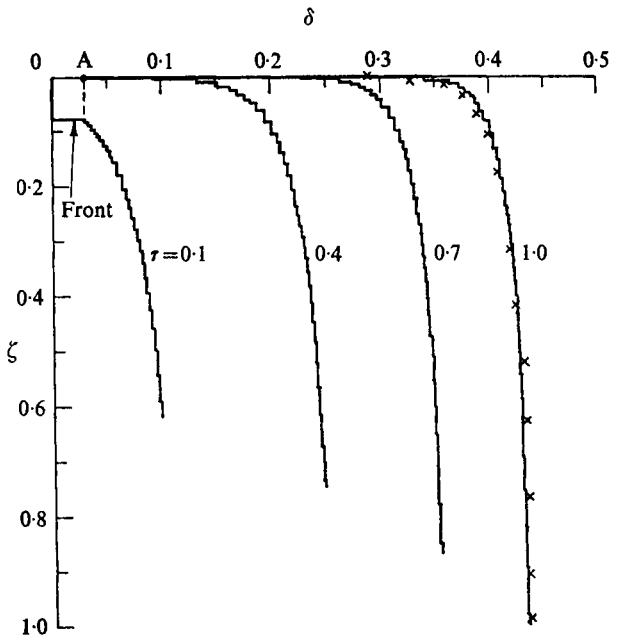

FIGURE 9. Computed tank stratification profiles in example §4.1 for various times τ, with α reduced to 0·057 near the free surface. (See figure 7 for other comments.) ×, experimental profile at $\tau = 1$.

computed and experimental profiles of δ at $\tau = 1$ agree quite well, except on and near the free surface. On the free surface ($\zeta = 0$), the experimental value of δ is 0·287, while the computed value is equal to zero: the front never gets to the free surface. Near the free surface ($0 < \zeta \leqslant 0{\cdot}15$), the deviation of the experimental and computed profiles is as large as 10%; for $\zeta > 0{\cdot}15$, it is only of order 1%. Of course, good agreement between the computed and experimental results on, and very close to, the free surface ought not to be expected. For the mathematical model does not contain the surface entry effect (which must dominate mixing very near the free surface, even for vertical entry by the cargo jet), or the effect of the small flow-development region, through which the cargo jet is converted to a forced plume.

On the other hand, near the free surface, agreement between computed and experimental results can be improved by a more appropriate entrainment constant α in this region. It was pointed out earlier in this section that Fr is rather large, and as a consequence plume momentum changes very slowly near the free surface. In other words, near the free surface we have in this case something that behaves more like an ideal jet ($\alpha = 0{\cdot}057$) than an ideal plume ($\alpha = 0{\cdot}082$). By using 0·082 throughout the plume, we introduced too much entrainment near the free surface. Hence, the computed profile of δ near the free surface is not as gradual as the experimental.

One representation of α, more appropriate here, is that for an ideal jet near the free surface, and that for an ideal plume further down. Accordingly, we used in the computer program $\alpha = 0{\cdot}057$ from the free surface ($\zeta = 0$) down to a value

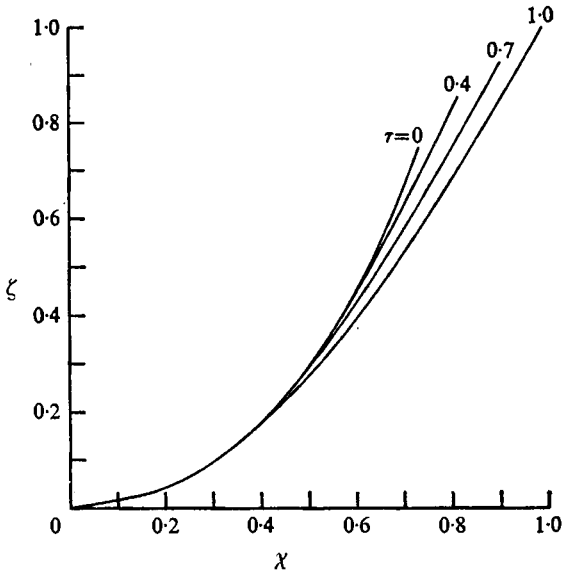

FIGURE 10. Plume trajectories of example §4.2 for various times τ.

of ζ at which the increase in m is within 10% of the value of m at $\zeta = 0$, and 0·082 from there on. The tank stratifications that resulted from this computation, together with the experimental results, are shown in figure 9. The agreement between computed and experimental results is now very good throughout the tank except, as expected, on and very close to the free surface. Their maximum deviation is within 2%, while their average deviation is only about 1%.

4.2. *Second example: bottom-fill, horizontal nozzle*

The cargo is lighter than the tank's inventory by 5·7% in this case, and is transferred through a horizontal nozzle placed flat on the bottom of the tank and directed toward its centre-line. The physical and normalized parameters of the case are summarized in table 1. For numerical reasons (stated in §2.3.1), $\theta_0 = 2°$ was used in the computer program instead of 0°. This does not introduce any significant uncertainties in the results: the actual orientation of the nozzle could very well be off the horizontal plane by 2°. Again, the tank is unstratified initially, and the reference density ρ_0 is taken equal to the inventory density, so that $\delta = 0$ at $\tau = 0$.

Figure 10 shows the normalized plume trajectories for various times. (Recall that, with bottom-fill nozzles, the origin of ζ is on the bottom of the tank and that, on completion of cargo transfer, the free surface is at $\zeta = 1$.) Evidently, the plume turns upward after a small distance from the nozzle exit, and its horizontal range is at no time larger than its height. The initial, almost horizontal jet is bent upward by the strong buoyant forces. Obviously, there is no way that the tank wall could interfere with the plume in this case. These statements on the trajectory of the plume were verified visually in the laboratory.

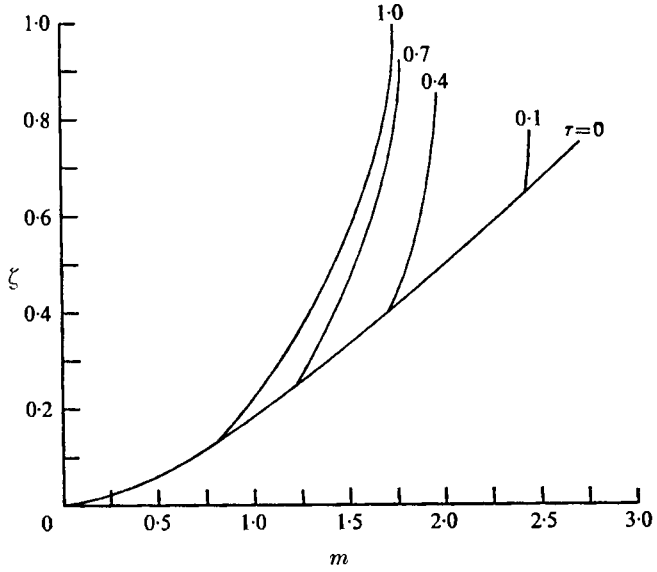

FIGURE 11. Example §4.2: flux of vertical momentum m against distance from tank bottom ζ for various times τ.

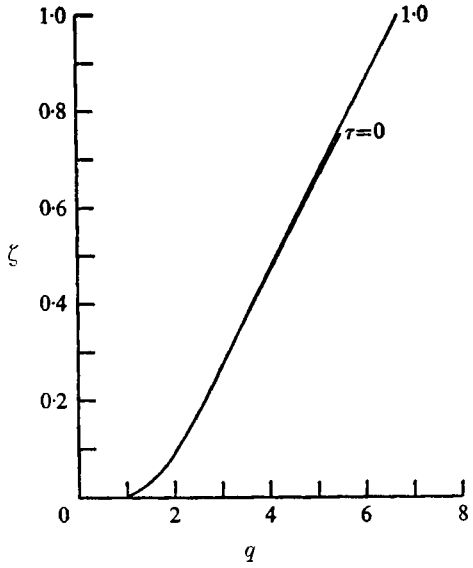

FIGURE 12. Example §4.2: volume flux q against distance from tank bottom ζ at the onset ($\tau = 0$) and after ($\tau = 1$) cargo transfer.

The strong effect of the buoyant forces can be seen also in figure 11, which shows the flux m of the vertical momentum of the plume. The flux of the horizontal momentum of the plume remains constant throughout the plume, as pointed out in §2.3.1; and it is roughly equal to 1 in normalized form. One may see from figure 11 that m, which starts from practically zero, becomes equal to the flux of horizontal momentum in the plume within a small distance from the bottom.

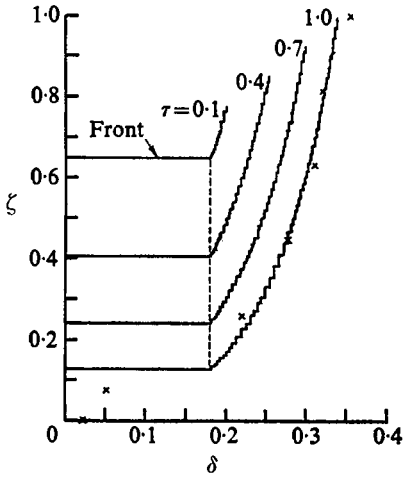

FIGURE 13. Computed tank stratification profiles in example §4.2 for various times τ. Tank bottom is at $\zeta = 0$. After cargo transfer ($\tau = 1$), free surface is at $\zeta = 1$. ×, experimental profile at $\tau = 1$.

At the free surface, m is 2·7 (at $\tau = 0$) to 1·7 (at $\tau = 1$) times the flux of horizontal momentum in the plume. The noticeable slope discontinuity in the m profile at the front is there because of the large discontinuity in f across the front. (See (12) and figure 14 below.)

One unexpected result in this case is that the volume flux q of the plume at a given height ζ hardly changes at all, as shown in figure 12, despite the fact that m at a given ζ does change with time considerably. (Equation (33) relates the variation of q with ζ to m.) It ought also to be noted that the values of q are an order of magnitude smaller than those in the first example. The main reason for this is that of the parameter β is almost an order of magnitude smaller. (See table 1.) Another reason is that the initial m is much smaller. In physical terms, there is much more entrainment of ambient liquid by the plume and, consequently, more mixing of the two liquids in the first example than in this.

The computed profiles of δ and f are shown in figures 13 and 14. Note the motion of the front toward the bottom of the tank. Note also that, as the front moves downward, the discontinuity of δ across the front does not change with time, while that of f does. The front moves much more slowly than in the first example. Even after cargo transfer, it is quite some distance from the bottom. At any given time, the tank liquid below the front consists entirely of the initial inventory (i.e. there is a sharp tank stratification until the front gets close to the bottom). It can be shown for this case too that an infinite time is required for the front to arrive exactly at $\zeta = 0$. Both the tardiness of the front and the rather large discontinuity in δ across the front (0·181) are, of course, due to the small q.

The experimental tank stratification after cargo transfer is also shown in figure 13. The stratification is stable here too; but there is more scatter in the experimental points than in the first example. The reason for the scatter is that this case is from an earlier series of experiments, in which the experimental technique was not as advanced as in the most recent series, from which the first example

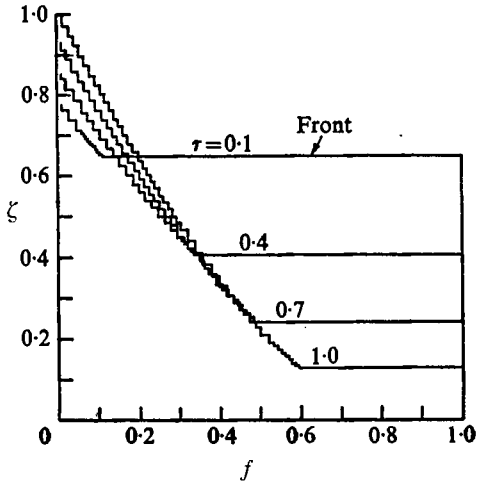

FIGURE 14. Example §4.2: buoyancy flux f against distance from the bottom of the tank ζ for various times τ.

comes. Considering the small scatter of the experimental results, we conclude that there is very good agreement between computed and experimental results throughout the tank, except in a region near the bottom (ζ less than about 0·2). Outside this region, the maximum deviation between computed and experimental results is within 4%, and the average deviation is less than 2%. This bottom region is roughly that occupied by the nozzle ($d/H_F = 0{\cdot}148$); and we should not expect our model to predict the tank stratification in this, the plume-flow development region. In fact, it is rather surprising that there is such good agreement between computation and experiment so close to the nozzle.

5. Concluding remarks

Except for some relatively minor, localized differences, the computed and experimental tank stratifications agree quite well. This establishes the validity of the mathematical model. The minor differences are due to local effects (such as the plume-flow development region, the entry of the cargo jet through the free surface, etc.). These are not included in the model; and they are so localized that they may be insignificant in practice.

This work has demonstrated the following. (i) The 'filling-box' model is valid for the circulation that results in the liquid in a finite tank when another liquid is injected into it through a nozzle. (ii) Well established entrainment theory for steady plumes is also applicable to time-dependent plumes in confined regions. (iii) Values of plume parameters α and λ used widely for steady plumes in environments of infinite extent are also approximately right for time-dependent plumes in confined regions. The emphasis in this last remark is on 'approximately', since the model is not extremely sensitive to α and λ.

The numerical method devised in this work is unique, in that it exploits the particular form of the governing differential equations. The method has worked in the computer program very stably and efficiently. In a disc-operated IBM

1130 with user core of only 4K, a rather small and slow computer, only a few minutes are required to run a case. A large number of cases have been run, and no instability or other numerical difficulties whatsoever have been encountered.

The efficiency and stability of the numerical method may be attributed to the fact that the method simulates the physical sequence of events rather closely. The discharge of the plume may be conceived of as taking place in a sequence of time intervals. Each interval creates a new layer of well-mixed liquid of a given density and height. After a layer is formed, it is convected vertically through the tank liquid because of plume entrainment. During this convection, the density of a given layer remains constant, but the height of the layer diminishes continuously, owing to depletion of the layer's liquid by plume entrainment. How much ambient liquid is entrained by the plume at any given time (and, most important, what kind) depends on where the various layers then are. Thus, the quantity and density of the liquid discharged by the plume are functions of time, and so are the height and density of the consecutive layers formed by the consecutive discharges of the plume. This sequence of events is precisely what the method simulates.

The raw data for the experimental results in the example of §4.2 are from experiments conducted by Mr D. A. Douglas, Department of Corporate Research, Cabot Corporation, prior to those of the author. The author is grateful to Professor K. A. Smith, Massachusetts Institute of Technology, for helpful discussions.

REFERENCES

BAINES, W. D. & TURNER, J. S. 1969 Turbulent buoyant convection from a source in a confined region. *J. Fluid Mech.* **37**, 51.

FAN, L. N. 1967 Turbulent buoyant jets into stratified or flowing ambient fluids. *W.M. Keck Lab. of Hydraulics and Water Resources, Calif. Inst. Tech. Rep. KH-R-15.*

FAN, L. N. & BROOKS, N. H. 1969 Numerical solutions of turbulent buoyant jet problems. *W. M. Keck Lab. of Hydraulics and Water Resources, Calif. Inst. Tech. Rep. KH-R-18.*

MORTON, B. R. 1959 Forced plumes. *J. Fluid Mech.* **5**, 151.

MORTON, B. R., TAYLOR, G. I. & TURNER, J. S. 1956 Turbulent gravitational convection from maintained and instantaneous sources. *Proc. Roy. Soc.* A **234**, 1.

ROUSE, H., YIH, C. S. & HUMPHREYS, H. W. 1952 Gravitational convection from a boundary source. *Tellus*, **4**, 201.

SMITH, K. A. & GERMELES, A. E. 1974 LNG tank stratification consequent to filling procedures. *Proc. 4th Int. Conf. on Liquified Natural Gas.*

TURNER, J. S. 1973 *Buoyancy Effects in Fluids.* Cambridge University Press.